PHYTOPLANKTON

The fate of photons absorbed by phytoplankton in the global ocean

Hanzhi Lin,[1]* Fedor I. Kuzminov,[1] Jisoo Park,[2] SangHoon Lee,[2] Paul G. Falkowski,[1,3]† Maxim Y. Gorbunov[1]†

Solar radiation absorbed by marine phytoplankton can follow three possible paths. By simultaneously measuring the quantum yields of photochemistry and chlorophyll fluorescence in situ, we calculate that, on average, ~60% of absorbed photons are converted to heat, only 35% are directed toward photochemical water splitting, and the rest are reemitted as fluorescence. The spatial pattern of fluorescence yields and lifetimes strongly suggests that photochemical energy conversion is physiologically limited by nutrients. Comparison of in situ fluorescence lifetimes with satellite retrievals of solar-induced fluorescence yields suggests that the mean values of the latter are generally representative of the photophysiological state of phytoplankton; however, the signal-to-noise ratio is unacceptably low in extremely oligotrophic regions, which constitute 30% of the open ocean.

For several decades, chlorophyll concentrations based on remotely sensed variations in ocean color have been used to derive global phytoplankton productivity (*1*, *2*). Primary productivity models implicitly include physiological processes, but their explicit representation has, thus far, been elusive (*3*, *4*). Variable chlorophyll fluorescence is the most sensitive, nondestructive signal detectable in the upper ocean that reflects instantaneous phytoplankton photophysiology (*5*–*7*). Over the past two decades, many hundreds of thousands of discrete in situ measurements of variable fluorescence have been made using ship-based active fluorometers. These instruments, primarily designed to quantify the quantum yield of photochemistry (F_v/F_m) (F_v, variable fluorescence; F_m, maximal fluorescence) in photosystem II (PSII), the reaction center responsible for splitting water, have been used to follow phytoplankton photophysiology in response to iron fertilization (*8*), across eddies (*9*, *10*), along meridional transects (*11*), and in response to many other phenomena (*12*, *13*). Although active variable fluorescence measurements have become almost routine, by themselves, they do not allow closure on the fate of light absorbed by phytoplankton. Here we report the fraction of sunlight absorbed by phytoplankton that is actually used to form chemical bonds in the global ocean. Further, we compare the spatial distributions of photochemical energy conversion to the pattern inferred from space-based retrievals of solar-induced fluorescence yields.

[1]Environmental Biophysics and Molecular Ecology Program, Department of Marine and Coastal Sciences, Rutgers, The State University of New Jersey, 71 Dudley Road, New Brunswick, NJ, USA. [2]Korea Polar Research Institute, 26 Songdomirae-ro, Yeonsu-Gu, Incheon, Republic of Korea. [3]Department of Earth and Planetary Sciences, Rutgers, The State University of New Jersey, Piscataway, NJ, USA.
*Present address: Institute of Marine and Environmental Technology, University of Maryland Center for Environmental Science, Baltimore, MD 21202, USA. **†Corresponding author. E-mail: falko@marine.rutgers.edu (P.G.F.); gorbunov@marine.rutgers.edu (M.Y.G.)**

The biophysical basis of fluorescence measurements derives from the three possible fates of solar energy absorbed by any photosynthetic organism (*14*). Absorbed photons can (i) generate photochemical reactions leading to the production of organic matter (with the rate k_p), (ii) be dissipated as heat (k_t), or (iii) be emitted back to the environment as fluorescence (k_f) (*15*). In a dark-adapted state or under low irradiance (when k_t is constant), the quantum yield of chlorophyll fluorescence, ϕ_f [$= k_f/(k_p + k_t + k_f)$], is inversely related to the quantum yield of photochemistry in PSII, $\phi_p = k_p/(k_p + k_t + k_f) = F_v/F_m$.

Substitution and rearrangement lead to

$$\phi_f = \phi_{fm}\,(1 - F_v/F_m) \qquad (1)$$

where ϕ_{fm} [$= k_f/(k_t + k_f)$] is the maximum fluorescence yield obtained when photochemistry is nil (e.g., at saturating background light).

This biophysical model predicts an inverse linear relationship between the quantum yield of photochemistry and that of chlorophyll fluorescence. However, by the early 1980s it was realized that exposure to high continuous irradiance can lead to a suite of thermal dissipative mechanisms, collectively called nonphotochemical quenching (NPQ) (*16*). These reactions markedly decrease the quantum yield of fluorescence at high background light. Hence, the relationship between chlorophyll fluorescence and photochemistry, described in Eq. 1, becomes highly nonlinear as NPQ phenomena play an increasingly larger role in energy dissipation.

Calculating the budget of absorbed solar radiation requires measurements of the quantum yields of at least two pathways; for example, photochemistry and fluorescence. Although the development and use of variable fluorescence techniques over the past two decades have provided unprecedented information about photochemical conversion in phytoplankton in situ, these instruments are unable to measure the absolute quantum yields of fluorescence. To overcome this basic limitation, we constructed an extremely sensitive sea-going instrument that measures chlorophyll fluorescence lifetimes in the picosecond time domain (*17*). The fluorescence lifetime can be quantitatively related to the absolute quantum yield of fluorescence (*18*)

$$\phi_f = \tau/\tau_n \qquad (2)$$

where τ_n is the intrinsic (or natural) lifetime constant for chlorophyll a molecules (*17*). Thus, the longer the lifetime, the higher the quantum yield of fluorescence.

Between 2008 and 2014, we obtained >150,000 discrete chlorophyll fluorescence lifetime measurements from the Pacific, Atlantic, Arctic, and Southern Oceans. These measurements constitute the map of quantum yields of chlorophyll fluorescence from phytoplankton in the upper

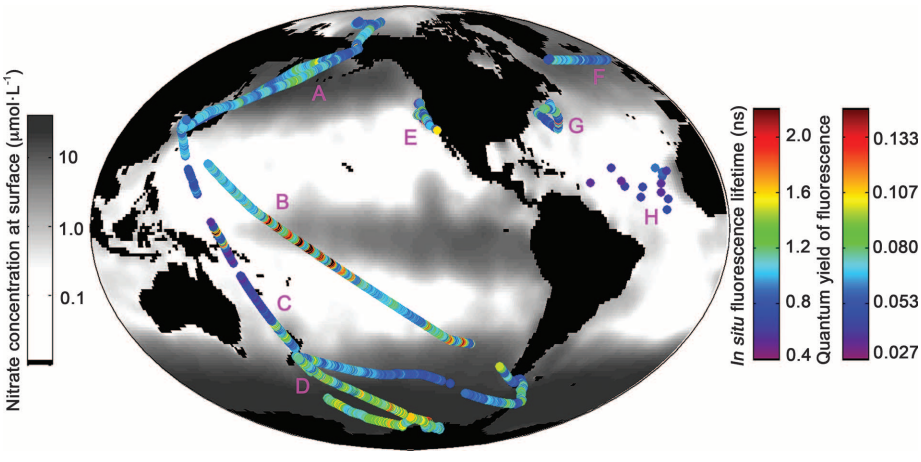

Fig. 1. Global distribution of ship-based measurements of chlorophyll fluorescence lifetimes and the derived quantum yields of fluorescence (Eq. 2) in the upper ocean, superimposed on the climatological map of surface nitrate concentrations in the world ocean (*32*). Periods of in situ sampling were (**A**) July–August 2011, (**B**) October–November 2011, (**C**) October–November 2010, (**D**) January 2012, (**E**) July 2014, (**F**) September 2010, (**G**) May 2014, and (**H**) August 2008.

ocean (Fig. 1). The nighttime in situ lifetimes ranged from 0.5 to 2.7 ns, with a mean of 1.13 ± 0.33 ns (Fig. 2). This naturally dark-adapted condition corresponds to a state in which all functional reaction centers are open and NPQ is absent. These values span the entire range of published lifetimes of in vivo chlorophyll fluorescence obtained from cultured phytoplankton (*17*) and reflect extraordinary variability in phytoplankton physiology in the global ocean. The general pattern of the fluorescence lifetimes in the central gyres of the global ocean is rather featureless, although phytoplankton growth is subject to both macro- and micronutrient limitation (*14*). The shortest fluorescence lifetimes (<1 ns) were observed along continental margins, in the Antarctic convergence, and in the subtropical Atlantic and Pacific oceans. These lifetime distributions support the hypothesis that phytoplankton in the central gyres are acclimated to broad scales and persistent nutrient limitation (*11*, *12*). In contrast, the longest fluorescence lifetimes were observed in high-nutrient–low-chlorophyll (HNLC) regions of the equatorial Pacific Ocean and the Southern Ocean, where primary production is limited by the paucity of iron (*19*), a micronutrient that is critical for the function of PSII (*20*, *21*). The exceptionally high values of fluorescence lifetimes in these areas of the global ocean are consistent with extremely

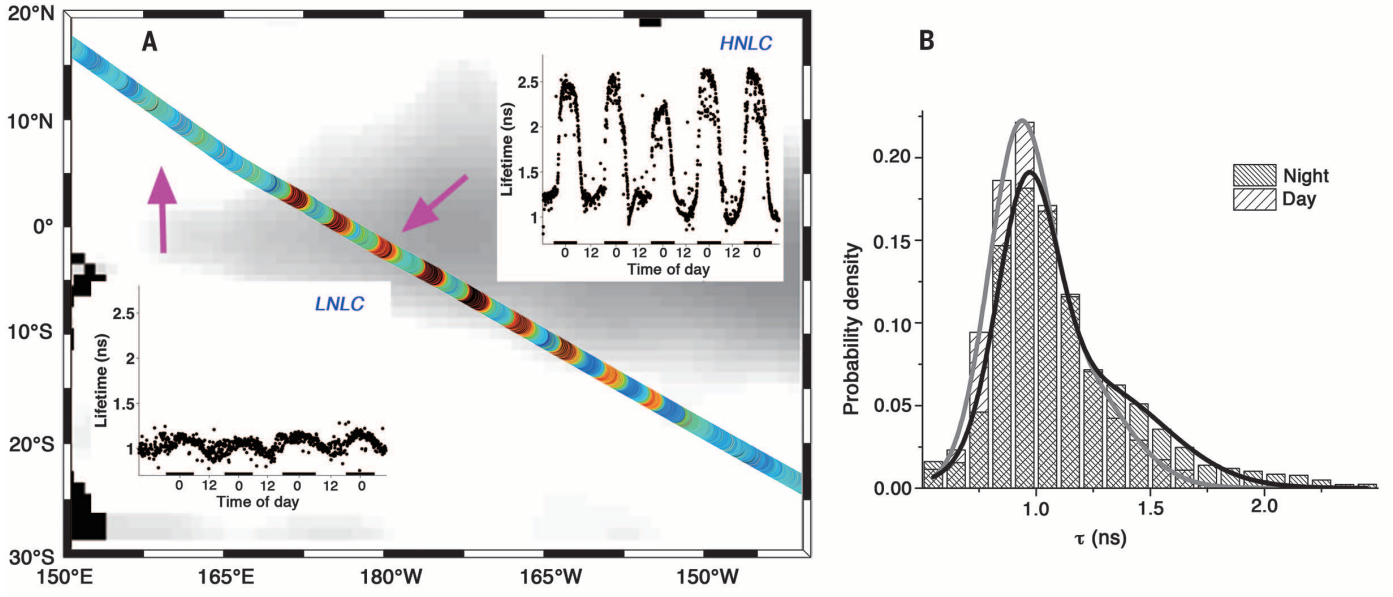

Fig. 2. (A) Representative diel cycles of chlorophyll fluorescence lifetimes in HNLC and LNLC regions of the Pacific Ocean obtained in October 2011. The color bar for lifetimes is the same as in Fig. 1. (**B**) Histograms of the fractional frequency of lifetime measurements in daytime and at night, respectively. The mean value of nighttime lifetimes is 1.13 ± 0.33 ns and that of daytime lifetimes is 1.02 ± 0.22 ns.

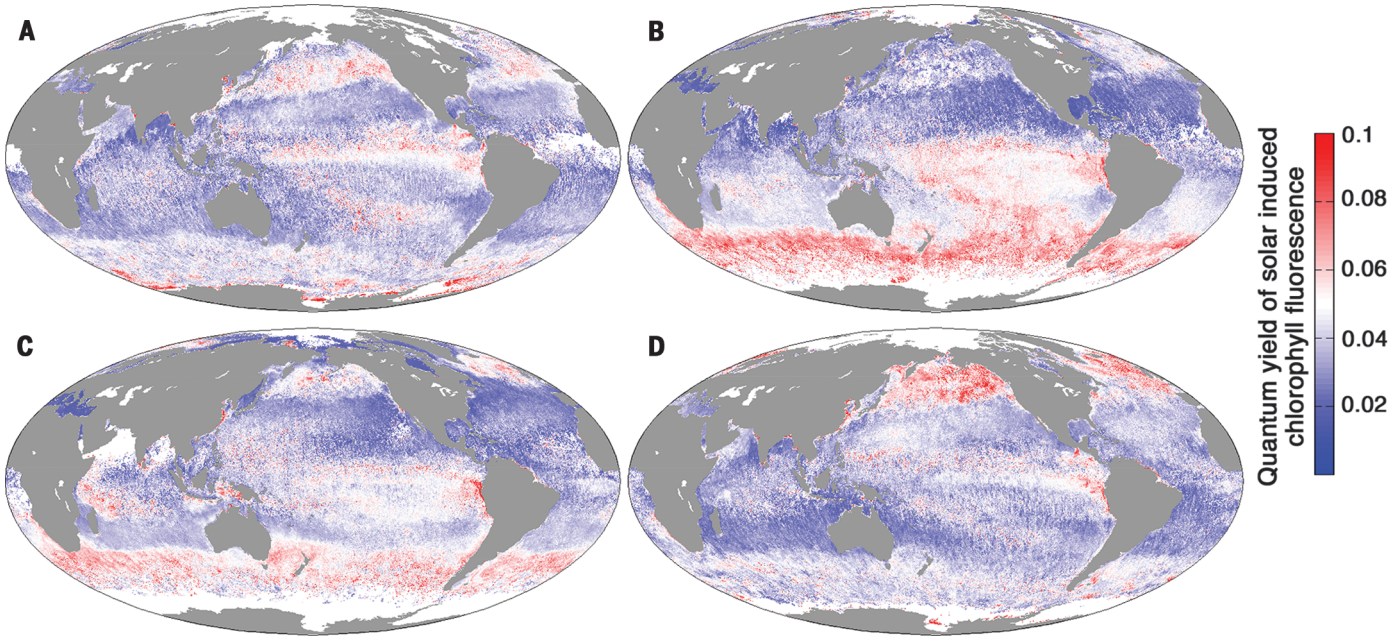

Fig. 3. Global seasonal maps of quantum yields of solar-induced chlorophyll fluorescence in the upper ocean. (**A**) Boreal winter (21 December 2011 to 20 March 2012); (**B**) boreal spring (21 March to 20 June 2012); (**C**) boreal summer (21 June to 20 September 2012); and (**D**) boreal autumn (21 September to 20 December 2012).

low F_v/F_m values and indicative of a large fraction of nonfunctional PSII reaction centers and energetically uncoupled antenna pigment-protein complexes (*21*–*23*).

There is a strong diel cycle in fluorescence lifetimes; in general, lifetimes were longer at night than during daytime, in spite of a marked reduction in the quantum yields of photochemistry under strong sunlight (Fig. 2). The more than fivefold variability in dark-adapted fluorescence lifetimes in situ far exceeds that predicted by Eq. 1. However, this dynamic range is greatly attenuated in high light, when NPQ processes are activated. For example, exceptionally long lifetimes (>2 ns) measured in a dark-adapted state in HNLC regions decrease by more than twofold in high light, whereas relatively short lifetimes (~1 ns) in low-nutrient–low-chlorophyll (LNLC) regions decrease by only 30% under the same conditions (Fig. 2A). Regardless of the molecular mechanisms responsible for NPQ, the net result for high light conditions is increased thermal dissipation of absorbed light in PSII, leading to both reductions in photochemical energy conversion efficiency and in the range of variability of the quantum yields of fluorescence.

With the launch of the Moderate Resolution Imaging Spectroradiometer (MODIS) and Medium Resolution Imaging Spectrometer (MERIS) satellites, which possess the capability of remotely detecting solar-induced chlorophyll fluorescence signals from the global ocean, it became theoretically possible to calculate the quantum yield of chlorophyll fluorescence from space (*24*–*26*). However, the theoretical basis for estimating the relationship between chlorophyll fluorescence and photochemistry was developed before there was an understanding of NPQ (*24*). We therefore examined how the measured in situ fluorescence lifetimes are related to satellite-derived estimates of the quantum yield of chlorophyll a fluorescence.

Statistical analyses (effective sample size >20,000) by both Pearson's linear correlation coefficient and two nonparametric Kendall's tau and Spearman's rho coefficients revealed a weak linear correlation ($P < 0.01$) between these satellite-derived solar-induced fluorescence yields and the ship-based measurements (table S1). Satellite-based estimates of the quantum yield are derived from observations of the surface ocean at times close to local noon (*27*). Hence, the remotely sensed estimates inevitably are obtained at very high irradiances and are strongly influenced by NPQ, a phenomenon that is extremely difficult to quantify in global biophysical models. NPQ is not only critically dependent on pigment composition within the light-harvesting antennae of the phytoplankton (which, in turn, is affected by phytoplankton community composition), but also on upper ocean turbulence as it affects the light field experienced by the community (*28*), as well as nutrient stress (*19*). Despite these complications, qualitative comparison of satellite-derived maps of quantum yields of chlorophyll fluorescence (Fig. 3) reveals basic trends that often, but not always, correspond to in situ lifetime measurements. For example, in the Southern Ocean (an HNLC region), satellite-derived quantum yields are high and correlate with long lifetimes. In this iron-limited region of the world oceans, there is a well-documented reduction in photosynthetic energy conversion efficiency as a result of impairment of PSII reaction centers and potential energetic uncoupling of the antenna pigment-protein complexes (*7*, *22*). In the LNLC regions of the central oceanic gyres of the North and South Pacific and the North Atlantic, measured fluorescence lifetimes are significantly shorter than in HNLC regions. Although the mean fluorescence yield based on the satellite retrievals for the oligotrophic open ocean is 0.043 (Fig. 4) and is generally concordant with the values measured in situ, the high estimates of quantum yields obtained from the space-based platform (Fig. 3) are not corroborated by in situ lifetime measurements. Further, the range of estimated quantum yields derived from satellite-based measurements (more than sixfold) is far larger than that of the in situ lifetimes measured at high irradiances (about threefold). Indeed, the range of the estimated quantum yields of fluorescence in the global ocean (~0.02 to 0.15) appears to exceed that of our current biophysical understanding of photochemistry in phytoplankton. What might be the source of this discrepancy?

In the central ocean gyres, where surface chlorophyll concentrations are very low (<0.1 mg m^{-3}), the fluorescence signals propagated to space are extremely weak. As a result, the current algorithms used to calculate quantum yields of fluorescence become increasingly uncertain [Fig. 4 and (*26*, *29*)]. The relationship between measured lifetimes and satellite-derived quantum yields diverges. In contrast to the satellite-derived yields, which have significant "noise," the in situ lifetime measurements remain extremely precise (within 5%) even at the lowest chlorophyll concentrations found in the upper ocean. Another factor behind this discrepancy is the effect of pigment packaging within a phytoplankton cell (*25*, *30*, *31*), which is most pronounced in larger cells and reduces the observed quantum yields, as compared to their true "molecular" values inferred from lifetime measurements. Similarly, the uncertainties of the current algorithms for remote sensing retrievals of phytoplankton absorption coefficients (*25*) further reduce the accuracy of satellite-based estimates of the quantum yields.

Although quantum yields of chlorophyll fluorescence obtained from current satellite sensors

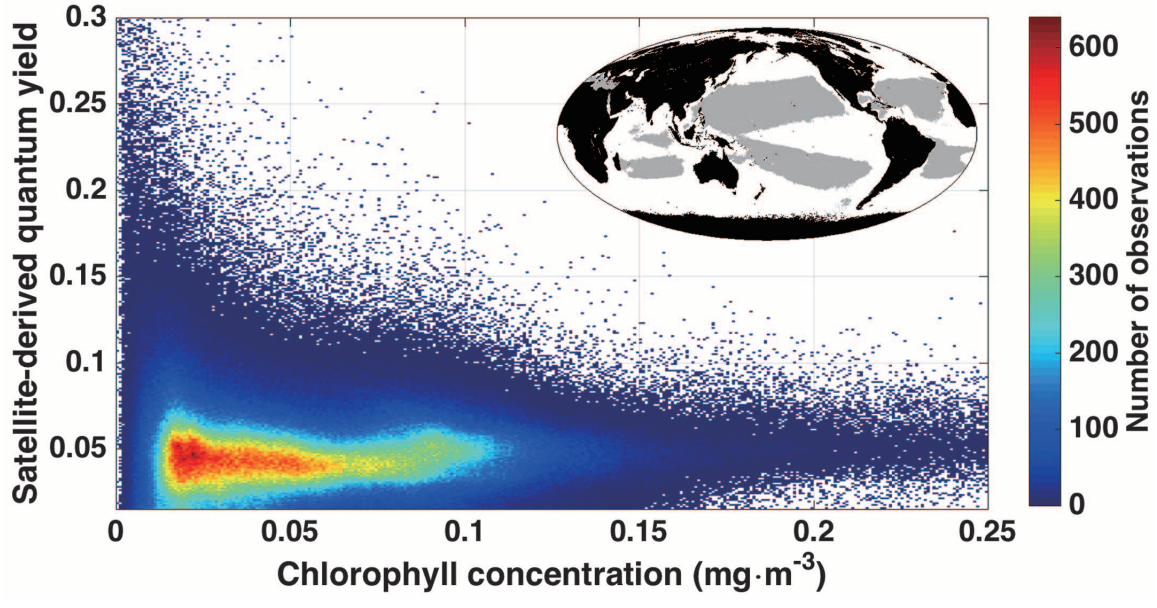

Fig. 4. Variations in MODIS retrievals of the quantum yields of chlorophyll fluorescence (sample size $n = 5.17 \times 10^6$) with chlorophyll abundance (*17*). The mean value of these satellite-derived quantum yields is 0.043. The average value of in situ lifetime measurements at noon (between 10 a.m and 2 p.m local time) is 0.99 ± 0.2 ns, which corresponds to the quantum yield of 0.066 ± 0.013. (**Inset, top right**) Global distribution (10-year average) of chlorophyll concentrations in the boreal summer. The gray area indicates oligotrophic regions with chlorophyll concentrations below 0.1 mg m_{-3}, this area covers ~30% of the global ocean.

have many inherent inaccuracies, this approach to understanding global photophysiology of phytoplankton should not be abandoned. We suggest that relating the space-based estimates to in situ measurements of chlorophyll fluorescence lifetimes will provide a pathway to understanding photobiological energy utilization and dissipation processes on a global scale. For example, the maximal average photochemical energy conversion efficiency (ϕ_P) at night in the global ocean, obtained simultaneously with our lifetime measurements, is 0.35 ± 0.11 (fig. S2). Given an average nighttime lifetime of 1.13 ns (Fig. 2), we deduce that thermal energy dissipation accounts for ~60% of the photosynthetically active quanta absorbed by phytoplankton globally. In contrast, under optimal growth conditions in the laboratory, an average phytoplankton cell uses ~65% of the absorbed quanta for photochemistry and dissipates <35% as heat. The fact that thermal dissipation of absorbed quanta by phytoplankton in the upper ocean is so high strongly implies that a large fraction of cells have impaired or nonfunctional PSII reaction centers and/or uncoupled photosynthetic antennae. We conclude that, although photochemical energy conversion to biomass in the oceans accounts for half of the global carbon fixed per annum, the overall energy conversion efficiency is relatively low and is limited by nutrient supply.

REFERENCES AND NOTES

1. D. Antoine, J. M. Andre, A. Morel, *Global Biogeochem. Cycles* **10**, 57–69 (1996).
2. C. B. Field, M. J. Behrenfeld, J. T. Randerson, P. Falkowski, *Science* **281**, 237–240 (1998).
3. M. J. Behrenfeld, E. Boss, D. A. Siegel, D. M. Shea, *Global Biogeochem. Cycles* **19**, GB1006 (2005).
4. M. J. Behrenfeld, P. G. Falkowski, *Limnol. Oceanogr.* **42**, 1–20 (1997).
5. P. G. Falkowski, Z. Kolber, *Aust. J. Plant Physiol.* **22**, 341–355 (1995).
6. Z. Kolber, P. G. Falkowski, *Limnol. Oceanogr.* **38**, 1646–1665 (1993).
7. G. H. Krause, E. Weis, *Annu. Rev. Plant Physiol.* **42**, 313–349 (1991).
8. P. W. Boyd *et al*., *Nature* **407**, 695–702 (2000).
9. T. S. Bibby, M. Y. Gorbunov, K. W. Wyman, P. G. Falkowski, *Deep Sea Res. Part II Top. Stud. Oceanogr.* **55**, 1310–1320 (2008).
10. P. G. Falkowski, D. Ziemann, Z. Kolber, P. K. Bienfang, *Nature* **352**, 55–58 (1991).
11. M. J. Behrenfeld *et al*., *Nature* **442**, 1025–1028 (2006).
12. D. J. Suggett, C. M. Moore, A. E. Hickman, R. J. Geider, *Mar. Ecol. Prog. Ser.* **376**, 1–19 (2009).
13. D. Tchernov *et al*., *Proc. Natl. Acad. Sci. U.S.A.* **101**, 13531–13535 (2004).
14. P. Falkowski, J. A. Raven, *Aquatic Photosynthesis* (Princeton Univ. Press, Princeton, NJ, ed. 2, 2007).
15. W. L. Butler, R. J. Strasser, *Proc. Natl. Acad. Sci. U.S.A.* **74**, 3382–3385 (1977).
16. M. Bradbury, N. R. Baker, *Proc. R. Soc. London Ser. B* **220**, 251–264 (1983).
17. Information on materials and methods is available on *Science* Online.
18. J. R. Lakowicz, *Principles of Fluorescence Spectroscopy* (Springer Science+Business Media, New York, ed. 3, 2006).
19. C. M. Moore *et al*., *Nat. Geosci.* **6**, 701–710 (2013).
20. J. A. Raven, M. C. W. Evans, R. E. Korb, *Photosynth. Res.* **60**, 111–150 (1999).
21. I. R. Vassiliev *et al*., *Plant Physiol.* **109**, 963–972 (1995).
22. P. G. Falkowski, R. M. Greene, R. J. Geider, *Oceanography* **5**, 84–91 (1992).
23. P. S. Schrader, A. J. Milligan, M. J. Behrenfeld, *PLOS ONE* **6**, e18753 (2011).
24. M. R. Abbott, R. M. Letelier, "Algorithm theoretical basis document: Chlorophyll fluorescence (MODros. Inf. Serv. Product Number 20)" (Ocean Biology Processing Group, NASA's Earth Observing System, 1999).
25. M. J. Behrenfeld *et al*., *Biogeosciences* **6**, 779–794 (2009).
26. Y. Huot, B. A. Franz, M. Fradette, *Remote Sens. Environ.* **132**, 238–253 (2013).
27. A. Savtchenko *et al*., *Adv. Space Res.* **34**, 710–714 (2004).
28. A. C. Alderkamp, H. J. W. de Baar, R. J. W. Visser, K. R. Arrigo, *Limnol. Oceanogr.* **55**, 1248–1264 (2010).
29. T. J. Browning, H. A. Bouman, C. M. Moore, *Global Biogeochem. Cycles* **28**, 510–524 (2014).
30. A. Bricaud, H. Claustre, J. Ras, K. Oubelkheir, *J. Geophys. Res. Oceans* **109**, C11010 (2004).
31. A. Morel, A. Bricaud, *Deep-Sea Res.* **28**, 1375–1393 (1981).

ACKNOWLEDGMENTS

We thank E. Boyle, P. Quinn, K. Thamatrakoln, and V. Fadeev for providing ship time and the captains and crews of research vessels *Oceanus*, *Knorr*, *Melville*, *Akademik Yoffe*, and *Araon*. This research was supported by grants NNX08AC24G from the NASA Ocean Biology and Biogeochemistry Program and SI-1334 from the Strategic Environmental Research and Development Program to M.Y.G. and P.G.F. H.L. and F.I.K. were supported by Institute of Marine and Coastal Sciences postdoctoral fellowships and the Bennett L. Smith Endowment to P.G.F. M.Y.G and F.I.K. were in part supported by grant 14-17-00451 from the Russian Science Foundation. J.P. and S.L. were supported by grant PP15020 from the Korea Polar Research Institute. All fluorescence data are deposited at PANGAEA (Publishing Network for Geoscientific and Environmental Data) under accession number PDI-11228.

SUPPLEMENTARY MATERIALS

www.sciencemag.org/content/351/6270/264/suppl/DC1
Materials and Methods
Figs. S1 to S4
Table S1
References (*32*–*52*)

30 March 2015; accepted 9 December 2015
10.1126/science.aab2213

NEURAL CIRCUITS

Inhibition protects acquired song segments during vocal learning in zebra finches

Daniela Vallentin,[1,2]* Georg Kosche,[1,2]* Dina Lipkind,[3] Michael A. Long[1,2]†

Vocal imitation involves incorporating instructive auditory information into relevant motor circuits through processes that are poorly understood. In zebra finches, we found that exposure to a tutor's song drives spiking activity within premotor neurons in the juvenile, whereas inhibition suppresses such responses upon learning in adulthood. We measured inhibitory currents evoked by the tutor song throughout development while simultaneously quantifying each bird's learning trajectory. Surprisingly, we found that the maturation of synaptic inhibition onto premotor neurons is correlated with learning but not age. We used synthetic tutoring to demonstrate that inhibition is selective for specific song elements that have already been learned and not those still in refinement. Our results suggest that structured inhibition plays a crucial role during song acquisition, enabling a piece-by-piece mastery of complex tasks.

Humans (*1*) and several other animal species (*2*–*4*) learn motor sequences by imitation. In the observer, a sensory percept must inform relevant motor circuits involved in the generation of the target behavior, but little is known about the neural mechanisms underlying this process. We address this issue in the male zebra finch, which acquires its courtship song by listening to (movie S1) (*5*) and imitating (*6*–*9*) a tutor. The forebrain nucleus HVC acts as an important sensorimotor interface because it receives direct connections from higher-order auditory centers (*10*–*12*) and generates commands essential for song production (*13*–*15*). In the juvenile zebra finch, tutor song exposure influences structural plasticity within HVC (*16*), a process that is thought to be crucial for song imitation (*17*). The tutor song has also been shown to drive network activity within HVC (*18*), but the responses of individual HVC premotor neurons during observational learning had not yet been explored.

We performed intracellular recordings in identified HVC neurons projecting to the robust nucleus of the arcopallium (RA) of 10 awake juvenile zebra finches during exposure to their tutor song. In 13 out of 29 of these HVC premotor neurons, tutor song playback caused spiking activity (Fig. 1, A to C). In those neurons, the timing of the evoked spikes was often highly precise across trials (see supplementary materials), demonstrating that exposure to the tutor song is sufficient to drive patterned spiking activity within HVC and may serve an instructive role for the developing HVC premotor circuit. We also observed reliably timed tutor-evoked spiking in RA (18 neurons in

[1]NYU Neuroscience Institute and Department of Otolaryngology, New York University Langone Medical Center, New York, NY 10016, USA. [2]Center for Neural Science, New York University, New York, NY 10003, USA. [3]Laboratory of Vocal Learning, Department of Psychology, Hunter College, New York, NY 10065, USA.
*These authors contributed equally to this work.
†Corresponding author. E-mail: mlong@med.nyu.edu